Consolidation Analysis of Soft Ground Improved by Stone Columns Incorporating Foundation Stiffness

Pei Tai

PhD (Wollongong)

Postdoctoral Research Fellow, Department of Civil and Environmental Engineering, School of Engineering, The Hong Kong University of Science and Technology, Clear Water Bay, Kowloon, Hong Kong

Buddhima Indraratna

PhD (Alberta), MSc (Lond.), BSc (Hons., Lond.), DIC, FIEAust., FASCE, FGS

Distinguished Professor of Civil Engineering, Faculty of Engineering and Information Sciences,

Director, Centre for Geomechanics and Railway Engineering; University of Wollongong, Wollongong City, NSW 2522, Australia

Cholachat Rujikiatkamjorn

BEng (Hons), MEng (AIT), PhD (Wollongong)

Associate Professor of Civil Engineering, Centre for Geomechanics and Railway Engineering, Faculty of Engineering and Information Sciences, University of Wollongong, Wollongong City, NSW 2522, Australia

Author for correspondence:

Prof. B. Indraratna
Faculty of Engineering
University of Wollongong
Wollongong, NSW 2522, Australia.
Ph: +61 2 4221 3046
Fax: +61 2 4221 3238
Email: indra@uow.edu.au

Submitted to: International Journal of Geomechanics (ASCE)

Consolidation Analysis of Soft Ground Improved by Stone Columns Incorporating Foundation Stiffness

Abstract

The consolidation of soft ground improved by stone columns is normally analysed under equal strain or free strain conditions. In this study a new consolidation model for stone columns is proposed to capture actual field conditions that lie between these two hypotheses, where a permeable foundation layer on top of the unit cell is introduced. By considering the stiffness of this layer, a closed-form solution can be derived, which indicates a considerable difference between the equal strain and free strain conditions. The influence of foundations with varying values of stiffness is examined, and the results demonstrate that as the foundation layer becomes stiffer, the time needed to achieve a 90% degree of consolidation decreases and so does the differential settlement, but the steady stress concentration ratio increases. This is also confirmed by a parametric study carried out under varying dimensionless ratios with respect to soil modulus, column spacing and permeability. A computational example is provided to show the implications of these results on actual design. Finally, a case study is presented to illustrate that the proposed model is able to provide more realistic predictions of settlement and stress concentrations on top of the unit cell.

Keywords: consolidation, stone column, differential settlement, stress concentration

Introduction

Conventional radial consolidation theory was first proposed by Barron (1948), to describe the cases of *equal strain* and *free strain*. For a unit cell which consists of homogeneous soil, *equal strain* condition assumes that the vertical strain is always uniform at a given depth as consolidation progresses, and therefore, the vertical stress on top of the unit cell is uneven. However, *free strain* condition imposes a uniform vertical stress at the top surface that results in differential settlement as consolidation takes place. Over the years, various solutions for radial consolidation with vertical drains have been developed by adopting these two concepts (Hansbo et al., 1981; Lei et al., 2015; Leo, 2004; Rujikiatkamjorn and Indraratna, 2014; Tang and Onitsuka, 1998; Walker and Indraratna, 2006; Zhu and Yin, 2001). For flexible prefabricated vertical drains, any difference in the average degree of consolidation based on either condition is found to be small, i.e., often within 5% (Richart, 1959; Zhu and Yin, 2004). Therefore, when designing vertical drains, either *equal strain* or *free strain* condition can be adopted.

For cases with stone columns, Han and Ye (2001) proposed a simplified method to estimate the average degree of consolidation of ground reinforced with stone columns that incorporates both well-resistance and soil disturbance. The behaviour of such a composite ground under time-dependent loading has been studied adopting an analytical approach by Wang (2009), while solutions that incorporate column deformation as well as combined vertical and radial flow have been discussed by Xie et al. (2009) and Lu et al. (2010). Indraratna et al. (2013) proposed a numerical solution for soft soil improved with stone column based on *free strain* by considering the effects of arching and clogging. Despite these efforts, there is still a large disparity among the aforementioned solutions, which clearly implies that when assumptions of *equal strain* and *free strain* are applied to a relatively stiff stone column system there can be a significant deviation (Han, 2014). Moreover, significant differential settlement which is likely to occur for nonuniformly distributed loading condition (Bouassida and Carter, 2014) also needs to be considered carefully.

In this paper, a modified consolidation model is presented where a theoretical condition between *equal strain* and *free strain* that captures the foundation stiffness is described. A closed-form analytical solution is obtained to calculate the average degree of consolidation, the redistribution of vertical stress, and the differential settlement between the column and the surrounding soil, supported by an illustrated example and a case study. A parametric study is also carried out to evaluate the effect of foundation stiffness.

Establishment of theoretical model

Basic assumptions

Unlike flexible vertical drains, the difference between the stiffness of a stone column and soil can lead to redistribution of stress and differential settlement between the top of the column and the soil, therefore, an assumption of either *free strain* or *equal strain* can be unrealistic. In order to address this dilemma, a mathematical model is proposed, where an additional layer is added on top of the original unit cell to represent the foundation or platform (Figure 1).

The proposed model is based on the following assumptions:

1) Darcy's law is valid.
2) Only vertical flow is considered inside the stone column, while only radial flow is accounted in the surrounding clay.
3) The top surface of the unit cell is free draining, but the bottom and the unit cell boundary are impermeable.
4) The load on top of the foundation is uniform and time independent (constant), and only the vertical strains are considered.
5) The pore water pressure and flow velocity are continuous across the column-soil interface.

6) The weight of the foundation layer and its compression are ignored.
7) Any possible shear stress at the column-soil interface is ignored while the shear stress in the foundation layer is calculated using a method that is analogous to the "trapdoor theory" by Terzaghi (1943) as elaborated later.

As shown in Figure 1, column settlement at the top surface of the unit cell can be treated as uniform, whereas the actual settlement on top of the surrounding soil depends on the radial distance (i.e., closer to the column means less settlement). The average vertical strains of the stone column (ε_c) and the surrounding soil (ε_s) are used after being determined from:

$$m_{vs}\frac{\partial[\sigma_s(t)-\bar{u}_s(z,t)]}{\partial t}=\frac{\partial\varepsilon_s(z,t)}{\partial t} \quad (1)$$

$$m_{vc}\frac{\partial[\sigma_c(t)-\bar{u}_c(z,t)]}{\partial t}=\frac{\partial\varepsilon_c(z,t)}{\partial t} \quad (2)$$

where σ_c and σ_s are the vertical stresses on top of the stone column and surrounding soil, respectively (no attenuation with depth), $\bar{u}_c$ and $\bar{u}_s$ are the average excess pore pressure in the stone column and surrounding soil, respectively, and m_{vc} and m_{vs} are the coefficients of volume compressibility of the stone column and surrounding soil, respectively.

Consideration of the foundation stiffness

The shear stress generated in the foundation layer may differ depending on the type of foundation material (e.g. concrete, sandy soil, or asphalt), and the nature of vertical stress redistribution such as arching; the latter often attracts a variety of opinions when included in modelling (Low et al., 1994; Madhav and Van Impe, 1994; Van Eekelen et al., 2013). In this study, shear stress at the overlying foundation is calculated based on the "trapdoor theory" initially proposed by Terzaghi (1943). It is assumed that when differential settlement occurs, any sliding in the foundation layer is vertical and the normal stress is uniform (Tien, 1996) as shown in Figure 2(a); this assumption has also been adopted in pile-embankment analysis (Chen et al., 2008). The generation of shear stress in the foundation layer is determined by mimicking a traditional direct shear test. A typical curve of shear stress versus the horizontal strain in a direct shear test is shown in Figure 2(b) (Ishibashi, 2011; Schofield and Wroth, 1968), and similarly, the shear stress (τ) at the sliding surface is related to the normal stress (σ_h) and the differential settlement (ΔS). Given that the allowable differential settlement of a foundation is usually restricted, it is reasonable to consider that the stress-strain curve would still be in the linear stage. Therefore, in the proposed model, shear stress in the foundation layer is assumed to be linearly proportional to its vertical strain. The slope of the stress-strain curve in a direct shear test defines its shear resistance, whereas in this model the slope of shear stress versus normalised differential settlement, $\Delta S/H_1$, is introduced as the stiffness of the foundation, denoted as K. This straight-forward way of considering shear stress may not reflect the real mechanism, but its simplicity enables the following coupled analysis to be carried out effectively.

By considering the force equilibrium in the foundation layer, the loads on top of the embankment should be equal to the supporting force provided at the top surface of the unit cell. The redistribution of vertical stress can then be calculated as follows ((3-5):

$$\pi(r_s^2 - r_c^2)\sigma_s(t) = \pi(r_s^2 - r_c^2)\sigma - \Delta\sigma \cdot H_1 \cdot \pi r_c \tag{3}$$

$$\pi r_c^2 \sigma_c(t) = \pi r_c^2 \sigma + \Delta\sigma \cdot H_1 \cdot \pi r_c \tag{4}$$

$$\frac{\int_0^H \varepsilon_s(z,t)dz - \int_0^H \varepsilon_c(z,t)dz}{H_1} K = \Delta\sigma \tag{5}$$

where r_c and r_s are the radius of the stone column and unit cell respectively, H_1 is the thickness of the foundation layer, K is the stiffness of the foundation, and $\Delta\sigma$ is the shear stress in the foundation layer.

The relationship between vertical strain and excess pore pressure can be represented by (6) and (7), and a detailed derivation is given in Appendix I. Through these two equations, the vertical strains can be calculated independent of the thickness of the foundation layer.

$$\frac{\partial \varepsilon_s}{\partial t}=\frac{m_{vc}m_{vs}KHr_c^2\frac{\partial \bar{u}_c}{\partial t}-m_{vs}(r_c^2-r_s^2)(m_{vc}HK+r_c)\frac{\partial \bar{u}_s}{\partial t}}{r_c^2[KH(m_{vc}-m_{vs})+r_c]-r_s^2(r_c+m_{vc}KH)} \tag{6}$$

$$\frac{\partial \varepsilon_c}{\partial t}=\frac{m_{vc}r_c(m_{vs}KHr_c+r_s^2-r_c^2)\frac{\partial \bar{u}_c}{\partial t}+m_{vc}m_{vs}KH(r_s^2-r_c^2)\frac{\partial \bar{u}_s}{\partial t}}{r_c^2[KH(m_{vc}-m_{vs})+r_c]-r_s^2(r_c+m_{vc}KH)} \tag{7}$$

where H is the thickness of the unit cell.

Governing equations

Deformation of the stone column and surrounding clay should be equal to the net flow into the system. Based on deformation-flow equilibrium, the governing equations for the consolidation of clay and column can be established, as represented by (8) and (9), respectively.

$$\frac{1}{\gamma_w r}\frac{\partial}{\partial r}\left(k_s f(r) r\frac{\partial u_s}{\partial r}\right)=-\frac{\partial \varepsilon_s}{\partial t} \tag{8}$$

$$\frac{2k_s}{\gamma_w r_c}\frac{\partial u_s}{\partial r}\bigg|_{r=r_c}+\frac{k_c}{\gamma_w}\frac{\partial^2 \bar{u}_c}{\partial z^2}=-\frac{\partial \varepsilon_c}{\partial t} \tag{9}$$

where u_s is the pore water pressure of a certain point in surrounding soil, $f(r)$ is a function of radius that describes variations in permeability in the surrounding soil which can used to represent the smear effect, k_c and k_s are the coefficients of permeability of the stone column and undisturbed soil respectively, and γ_w is the unit weight of water.

The boundary conditions are given by (13), thus:

$$\left.\frac{\partial u_s}{\partial r}\right|_{r=r_s} = 0 \tag{10}$$

$$u_s = \bar{u}_c(r = r_c) \tag{11}$$

$$\bar{u}_s(0,t) = \bar{u}_c(0,t) = 0 \quad (t > 0) \tag{12}$$

$$\frac{\partial \bar{u}_s(H,t)}{\partial z} = \frac{\partial \bar{u}_c(H,t)}{\partial z} = 0 \tag{13}$$

The excess pore water pressure at the top surface of the unit cell is prescribed by the following: when vertical loads are first applied the induced excess pore water pressure is assumed to be uniform in the unit cell and equal to the magnitude of external loads, but when consolidation commences the excess pore pressure is immediately dissipated to zero at the surface of the unit cell.

The initial condition can then be expressed by (14), hence:

$$\bar{u}_s(z,0) = \bar{u}_c(z,0) = \sigma \tag{14}$$

Finally, a governing equation specifying the variable, $\bar{u}_c$, can be obtained, and the details of its derivation are given in Appendix II extending the past procedures (Lu et al., 2010; Tai et al., 2017).

$$C \cdot E \frac{\partial^3 \bar{u}_c}{\partial z^2 \partial t} - E \frac{\partial^2 \bar{u}_c}{\partial z^2} + (B + C \cdot D) \frac{\partial^2 \bar{u}_c}{\partial t^2} + (1 - D) \frac{\partial \bar{u}_c}{\partial t} = 0 \tag{15}$$

Analytical solutions

It is assumed that the excess pore water pressure in the stone column can be rewritten as a product of two independent functions (16), each with only one variable. Then, the governing equation obtained can be solved by the variable separation method, where:

$$\bar{u}_c = G(t) \cdot Z(z) \tag{16}$$

The governing equation can now be transformed into two ordinary differential equations (ODEs) as shown below:

$$-\frac{(B + C \cdot D)G''(t) + (1 - D)G'(t)}{C \cdot E \cdot G'(t) - E \cdot G(t)} = \frac{Z''}{Z} = -\alpha^2 \quad (\alpha > 0) \tag{17}$$

where α is a positive constant that will be explained later.

General solution

By considering Eqn. (17) as a second order linear ODE, its boundary condition and initial condition are represented by:

$$\bar{u}_c(0, t) = G(t)Z(0) = Z(0) = 0 \tag{18}$$

$$\bar{u}_c(z, 0) = G(0)Z(z) = \sigma \tag{19}$$

$$\frac{\partial \bar{u}_c(h, t)}{\partial z} = G(t)Z'(H) = Z'(H) = 0 \tag{20}$$

The solutions can then be obtained after finding Eigenfunctions based on the variable separation method (Kreyszig, 1988).

$$\bar{u}_c = \sum_n G(t) \cdot Z(z) \qquad (n = 1,2,3,\dots) \tag{21}$$

$$Z_n(z) = \sin(\alpha_n \mathrm{z}) \tag{22}$$

$$G_n(t) = b_n \mathrm{e}^{\beta_n \cdot t} + c_n \mathrm{e}^{\theta_n \cdot t} \tag{23}$$

$$\alpha_n = \frac{(2n-1)\pi}{2H} \tag{24}$$

$$\beta_n = \frac{-1 + D + CE\alpha_n^2 - \sqrt{-4(B+CD)E\alpha_n^2 + (1 - D - CE\alpha_n^2)^2}}{2(B+CD)} \tag{25}$$

$$\theta_n = \frac{-1 + D + CE\alpha_n^2 + \sqrt{-4(B+CD)E\alpha_n^2 + (1 - D - CE\alpha_n^2)^2}}{2(B+CD)} \tag{26}$$

In the above, the coefficients "b_n", and "c_n" are integration constants.

The excess pore water pressure in the stone column and surrounding soil can be written respectively as follows:

$$\bar{u}_c = \sum_1^n (b_n \mathrm{e}^{\beta_n \cdot t} + c_n \mathrm{e}^{\theta_n \cdot t}) \sin(\alpha_n \mathrm{z}) \tag{27}$$

$$\begin{aligned} \bar{u}_s = \sum_1^n &[b_n\,[1 + (CD+B)\beta_n - CE\alpha_n^2]\mathrm{e}^{\beta_n \cdot t} \\ &+ c_n[1 + (CD+B)\theta_n - CE\alpha_n^2]\mathrm{e}^{\theta_n \cdot t}] \sin(\alpha_n \mathrm{z}) \end{aligned} \tag{28}$$

In Eqn. (27) and (28), these two integration constants, b_n and c_n, can be determined by considering the initial condition ((14), hence:

$$b_n = \frac{\sigma(-1 + D - CE\alpha_n^2 + \sqrt{-4(B+CD)E\alpha_n^2 + (1 - D - CE\alpha_n^2)^2})}{\alpha_n H \sqrt{-4(B+CD)E\alpha_n^2 + (1 - D - CE\alpha_n^2)^2}} \tag{29}$$

$$c_n = \frac{\sigma\left(1 - D + CE\alpha_n^2 + \sqrt{-4(B + CD)E\alpha_n^2 + (1 - D - CE\alpha_n^2)^2}\right)}{\alpha_n H\sqrt{-4(B + CD)E\alpha_n^2 + (1 - D - CE\alpha_n^2)^2}} \tag{30}$$

The average degree of consolidation for the whole unit cell, $\overline{U}$, can then be calculated using:

$$\overline{U} = 1 - \frac{\left(1 - \frac{r_c^2}{r_s^2}\right)\bar{u}_s + \frac{r_c^2}{r_s^2}\bar{u}_c}{\sum_1^n \alpha_n \sin(\alpha_n \mathrm{z})\,\sigma H} \tag{31}$$

The vertical strains of stone column and surrounding soil can be calculated according to (6) and (7) together with the initial condition, which gives:

$$\varepsilon_s = \frac{m_{vc}m_{vs}KHr_c^2(\bar{u}_c - \sigma) - m_{vs}(r_c^2 - r_s^2)(m_{vc}HK + r_c)(\bar{u}_s - \sigma)}{r_c^2[KH(m_{vc} - m_{vs}) + r_c] - r_s^2(r_c + m_{vc}KH)} \tag{32}$$

$$\varepsilon_c = \frac{m_{vc}r_c(m_{vs}KHr_c + r_s^2 - r_c^2)(\bar{u}_c - \sigma) + m_{vc}m_{vs}KH(r_s^2 - r_c^2)(\bar{u}_s - \sigma)}{r_c^2[KH(m_{vc} - m_{vs}) + r_c] - r_s^2(r_c + m_{vc}KH)} \tag{33}$$

The stress concentration ratio, n_s, can now be calculated from:

$$n_s(t) = \frac{m_{vs}\int_0^H \varepsilon_c(z,t)dz + m_{vc}m_{vs}\int_0^H \bar{u}_c(z,t)dz}{m_{vc}\int_0^H \varepsilon_s(z,t)dz + m_{vc}m_{vs}\int_0^H \bar{u}_s(z,t)dz} \tag{34}$$

The differential settlement on the top surface of the unit cell, ΔS, now becomes:

$$\Delta S(t) = \int_0^H \varepsilon_s(z,t)dz - \int_0^H \varepsilon_c(z,t)dz \tag{35}$$

Equal strain condition

The equal strain hypothesis is valid when the stiffness of the foundation approaches infinity ($K \rightarrow +\infty$), and there is no differential settlement occurring during the whole consolidation process.

This means the governing equation can degenerate into the form shown below, whereby:

$$CE\frac{\partial^3 \bar{u}_c}{\partial z^2 \partial t} - E\frac{\partial^2 \bar{u}_c}{\partial z^2} + (1-D)\frac{\partial \bar{u}_c}{\partial t} = 0 \tag{36}$$

$$\bar{u}_s = \bar{u}_c + CE\frac{\partial^2 \bar{u}_c}{\partial z^2} \tag{37}$$

$$\frac{\partial \varepsilon_s}{\partial t} = \frac{\partial \varepsilon_c}{\partial t} = -\frac{r_c^2\frac{\partial \bar{u}_c}{\partial t} + (r_s^2 - r_c^2)\frac{\partial \bar{u}_s}{\partial t}}{(r_s^2 - r_c^2)/m_{vs} + r_c^2/m_{vc}} \tag{38}$$

Note that the secondary differential item for time has been cancelled, so the two ODEs after variable separation become:

$$\frac{(D-1)G'(t)}{C \cdot E \cdot G'(t) - E \cdot G(t)} = \frac{Z''}{Z} = -\alpha^2(\alpha > 0) \tag{39}$$

Through a similar procedure as obtaining the general solution, the solutions for the average excess pore pressure and vertical strain of a unit cell under equal strain condition can be derived as:

$$\bar{u}_c = \sum_1^n \frac{2\sigma r_s^2}{H[CE\alpha_n^3(r_c^2 - r_s^2) + \alpha_n r_s^2]} e^{\frac{E\alpha_n^2 t}{-1+D+CE\alpha_n^2}} \sin[\alpha_n z] \tag{40}$$

$$\bar{u}_s = (1 - CE\alpha_n^2)\bar{u}_c \tag{41}$$

$$\varepsilon_s = \varepsilon_c = -\frac{r_c^2\bar{u}_c + (r_s^2 - r_c^2)\bar{u}_s - \sigma r_s^2}{(r_s^2 - r_c^2)/m_{vs} + r_c^2/m_{vc}} \tag{42}$$

The stress concentration ratio can still be determined using Eqn. (34).

Free strain condition

The free strain hypothesis means that the stiffness of the foundation is negligible and the vertical stress on top of the unit cell is uniform. Consequently, the differential settlement only depends on the compression modulus of stone column and the surrounding soil, hence:

$$m_{vs}\frac{\partial(\sigma - \bar{u}_s)}{\partial t} = \frac{\partial \varepsilon_s}{\partial t} \tag{43}$$

$$m_{vc}\frac{\partial(\sigma - \bar{u}_c)}{\partial t} = \frac{\partial \varepsilon_c}{\partial t} \tag{44}$$

The structure of the degenerated equation for free strain is still the same as that of the general form, but with the two parameters B and K equalling zero, as represented by Eqns. (45)-(46). Therefore, the solution remains the same as the general one given earlier.

$$C \cdot E\frac{\partial^3\bar{u}_c}{\partial z^2 \partial t} - E\frac{\partial^2\bar{u}_c}{\partial z^2} + C \cdot D\frac{\partial^2\bar{u}_c}{\partial t^2} + (1 - D)\frac{\partial \bar{u}_c}{\partial t} = 0 \tag{45}$$

$$\bar{u}_s = \bar{u}_c + C \cdot D\frac{\partial \bar{u}_c}{\partial t} + C \cdot E\frac{\partial^2\bar{u}_c}{\partial z^2} \tag{46}$$

Comparison with previous studies

In order to verify the proposed model, comparisons are made with existing consolidation models under the hypotheses of *equal strain* (Han and Ye 2001, Lu et al. 2010) and *free strain* (Indraratna et al. 2013).

The basic parameters adopted in the verification are cited from Indraratna et al. (2013) and presented in Table 1. The smear effect can be considered by the permeability variation funtion *f(r)* in Eqn. (8), but the effect of clogging in the stone column is ignored. Meanwhile, the time factor, *T*, is adopted as the abscissa that can be defined as shown below.

$$T = \frac{k_s t}{4 m_{vs} \gamma_w r_s^2} \tag{47}$$

Figure 3 shows the comparison of the average degree of consolidation for a unit cell calculated using the proposed model with previous studies. The difference among the three curves of equal strain is negligible, which indicates that ignoring vertical flow in the surrounding soil and radial flow in the column is acceptable for a thick unit cell (>16m). However, with free strain, the consolidation predicted by the current model is much faster when the time factor is less than 0.1; the trend then reverses, and the degree of consolidation given by Indraratna et al. (2013) becomes higher at the later stage.

Differences between equal strain and free strain

The curves in Figure 3 also show that the degree of consolidation for free strain is higher than that for equal strain at the beginning, but then it falls behind at a later stage. This observation agrees with the statement made by Zhu and Yin (2004), except that the difference is rather small (<6%) for vertical drains in their analysis, whereas it can be up to 15% for stone columns. It can be concluded that, there is a large disparity in the consolidation rate of ground improved by stone columns that results from the basic hypotheses: whether *equal strain* or *free strain* is adopted.

There is also no redistribution of vertical stresses on top of the column and surrounding soil under *free strain* conditions, so the stress concentration ratio is always equal to 1, whereas the distribution of vertical stress for equal strain changes as consolidation progresses, as shown in Figure 4(a). Initially, most of the vertical loading is carried by the surrounding soil, so the vertical stress ratio on top of the stone column remains at a relatively low level, while the vertical stress ratio on the surrounding soil is larger than unity to maintain the force equilibrium. As consolidation continues, the vertical stress in the surrounding clay decreases while that on the stone column increases, and this agrees with the findings of Han and Ye (2001). Meanwhile, because of the assumption of equal strain, the stress concentration ratio will increase with consolidation until it reaches the same value as the compressibility ratio of the column material to the soil (i.e., 7 in this case), as shown in Figure 4(b).

The evolution of excess pore pressure in the surrounding soil and stone column under both hypotheses is presented in Figure 5(a) and 5(b), respectively. In the surrounding soil the initial excess pore pressure is higher, and its dissipation is faster for the case of equal strain. On the contrary, for the pore pressure in the stone column, the initial value under free strain is markedly higher than that of equal strain, but the difference between *equal strain* and *free strain* quickly becomes negligible.

Figure 6 gives the profiles of excess pore pressure at different times for stone column and surrounding soil, respectively. Echoing with Figure 5, Figure 6 also shows that the initial excess pore pressure decreases with depth in the surrounding soil, but it increases with depth in the stone column. It is also indicated that more time is required for the completion of consolidation under *free strain* conditions. When consolidation commences (T=0.001), the excess pore pressure ratio at the bottom of stone column is almost 0.8 for *free strain* and less than 0.4 for *equal strain* (Figure 6a), but after a short period of time (T=0.1), the pore pressure ratio in the stone column decreases to about 0.2 for both *equal strain* and *free strain*. Unlike *equal strain*, the amount of pore pressure dissipated in stone column is much higher for *free strain* when the time factor reaches 0.01, which explains why the degree of consolidation under *free strain* is higher initially. The initial excess pore pressure ratio in the surrounding soil is higher (larger than 1) for *equal strain* which again confirms the fact that the external load is mostly carried by the surrounding soil at the beginning (Figure 6b). However, the excess pore pressure in the surrounding soil is lower for *equal strain* when T equals to 0.01, which means that *equal strain* induces faster consolidation. Figure 6 also demonstrates that the excess pore pressure in the surrounding soil is not as sensitive to depth as it is in stone column, possibly due to the ignorance of vertical flow in surrounding soil. Note that the small variation with depth is attributed to the pore pressure gradient in stone column.

Effect of foundation stiffness

In practice, the stiffness of a foundation is neither infinity nor zero, therefore, the performance of soft ground improved by stone columns should be between *equal strain* and *free strain*. By varying the stiffness of the foundation, this behaviour can be captured by the proposed consolidation model. A parametric study was carried out to investigate the effect of foundation stiffness on the stone column, and the same parameters provided in Table 1 were used, except for the stiffness of foundation.

By considering the foundation layer as a common earth structure, the stiffness of the foundation layer can be determined based on direct shear tests of its base soil, while the typical values of stiffness, K, can be calculated from the existing direct shear tests that are listed in Table 2. As for a 2-3m high embankment, the lateral earth pressure is limited, and therefore, the resulting K value is expected to be relatively low. In the following analysis, the foundation stiffness was altered by using the compressibility of the surrouding soil as a reference; the product of foundation stiffness and volume compressibility ($K \cdot m_{vs}$) varies from 0.1 to 10, which corresponds to a stiffness of 200 kPa to 20,000 kPa.

Figure 7(a) shows that the change in foundation stiffness affects the consolidation rate. Initially, the rate decreases as the foundation stiffness increases, but after a certain time ($T \approx 0.03$) the consolidation accelerates when the foundation becomes stiffer, and cases of *equal strain* and *free strain* become the upper and lower boundary.

Naturally, the stress concentration ratio on top of the unit cell is also influenced by the stiffness of the foundation, as shown in Figure 7(b). The external loading is initially carried by the surrounding soil, but as consolidation progresses it is gradually transferred to the stone column. The stress concentration ratio approaches a steady value when consolidation approaches to the end. The steady stress concentration ratio increases as the foundation become stiffer, and in this case the steady stress concentration ratio is 7 (corresponding to the *equal strain* condition).

The differential settlement ratio ($\Delta S/H$) is defined as the ratio of differential settlement at the top of the unit cell to the height of the unit cell. Figure 7(c) shows that less differential settlement is generated as the foundation becomes stiffer. For a flexible foundation, negative differential settlement (around 2%) develops initially which means the column settles more than the surrounding soil at the beginning due to its high permeability, but then this trend reverses until the differential settlement becomes positive and finally reaches a steady value. This can be explained as follows: the excess pore pressure in the surrounding soil takes much longer to dissipate than inside the stone column, therefore, the compression of surrounding soil develops much slower than that of stone column, and the surrounding soil settles more than the column initially. Figure 7(c) also indicates that the differential settlement ratio can be negligible when the foundation is stiff, but it could be up to 18% when the foundation is flexible. Note that this amount of differential settlement is not realistic in field conditions because of the resistance mobilised at the column-soil interface, but the results presented hereby still highlight the need to evaluate the differential settlement.

Effect of modulus ratio, spacing ratio, and permeability ratio

The sensitivity of the modulus ratio, the permeability ratio of column material to soil, and column spacing are also studied under conditions between *equal strain* and *free strain*. Slightly different from the previous section, in this part, the stiffness of foundation is assigned as 1000, 2000 and 4000kPa, respectively (corresponds to the $K \cdot m_{vs}$ values of 0.5, 1, 2).

The quality (modulus) of stone column is crucial for the performance of the improved soft ground (Deb and Behera, 2016; Raju and Sondermann, 2005). In practice, the modulus ratio of column to clay is in the range of 10-40 (Hu, 1995, Kelly, 2014). Based on elastic theory, the coefficient of volume compressibility, m_v, can be calculated using Poisson's ratio, v, and Young's modulus, E_0 from the equation given below (Han and Ye, 2001).

$$m_v = \frac{(1+v)(1-2v)}{E_0(1-v)} \tag{48}$$

Han and Ye (2001) also suggested that the Poisson's ratios for stone column and surrounding soil should be chosen as 0.15 and 0.45, respectively. As a result, the ratio of coefficient of compressibility of clay to column is in the range of 2 to 11 when the modulus ratio of column to clay varies between 8 and 40.

The influence of modulus ratio under various values of foundation stiffness is investigated and the corresponding results are shown in Figure 8. The steady stress concentration ratio under different modulus ratios is compared to previous predictions (Barksdale and Bachus, 1983, Han and Ye, 2001) in Figure 8(a), and it is observed that these results follow a similar trend except that the current model shows slight nonlinearity. It is also noted that the steady stress concentration ratio increases with an increase in either modulus ratio or foundation stiffness, but the effect of foundation stiffness becomes negligible when the modulus ratio is relatively small (i.e. <10).

The time factor corresponding to 90% degree of consolidation, U_{90}, is usually used as an indicator to compare the consolidation rate among different cases. Figure 8(b) illustrates that U_{90} decreases as the modulus ratio increases or the foundation becomes stiffer. When the modulus ratio is less than 10, the value of U_{90} is not sensitive to the foundation stiffness.

Note that the differential settlement ratio increases with an increase in the modulus ratio, but it decreases as the foundation becomes stiffer, as shown in Figure 8(c). The differential settlement is likely to be affected significantly by the stiffness of foundation even at a relatively low modulus ratio (i.e. <10). Similarly, the radius ratio of unit cell to column (r_s/r_c) and the permeability ratio of column material to clay (k_c/k_s) are also varied under different values of stiffness of foundation. The radius ratio changes in the range of 1.5-3.5 while the permeability ratio varies between 10^3 and 10^6, both of which are in the typical range (Hu, 1995; Kelly, 2014). Only U_{90} is calculated to show the change of consolidation rate, as the stress concentration and differential settlement are unlikely to be affected significantly in this scenario. Figure 9(a) shows that U_{90} is normally higher for a larger radius ratio, and its value also increases slightly as the foundation becomes stiffer under a certain radius ratio. Figure 9(b) illustrates that further increase in the permeability ratio beyond 10^4 barely accelerates consolidation anymore, and U_{90} is not sensitive to the stiffness of the foundation at a given permeability ratio.

Practical design illustrative example

An example is given to illustrate how this proposed model can be used for a practical design. In a project where 0.8m diameter stone columns are spaced 2m apart in a rectangular pattern are used to stabilise a 10-meter-thick layer of soft clay over an impervious rock bed. Then it can be determined that the equivalent radius of the unit cell is 2.26m, which is 1.13 times of the column spacing, and an annular area outside the stone column with a diameter of 0.92m is disturbed due to installation. The permeability of undisturbed clay, disturbed clay, and column material are 10^{-9}, 10^{-10}, and 10^{-4}m/s, respectively. The coefficient of volume compressibility of column material and clay are 0.08 and 0.8 MPa^{-1}, respectively. The stiffness of foundation is 2,000kPa. A 100kPa vertical load is applied instantly and the degree of consolidation after 30 days and the time to achieve 90% of consolidation degree (U_{90}) are required. The proposed model predicts that the degree of consolidation after 30 days is 53.2% and U_{90} takes around 95 days. In comparison, the model of Han and Ye (2002) shows that the degree of consolidation after 30 days is 66.5% and U_{90} is 63 days, whereas Lu et al. (2010)'s model predicts that the 30-day degree of consolidation is 60% and U_{90} can be achieved within 79 days.

Application to a case study

In mid-2012 at the Ballina national field test facility, NSW, Australia, a group of stone columns were installed to improve the local soft clay. These fully-penetrated stone columns were in a square pattern at a spacing of 2-metre. Subsequently a 4m high embankment was built in four stages within 50 days. The first metre of the embankment consisted of rockfill overlain with a layer of geogrid; the natural unit weight of embankment fill was between 17.5-20kN/m^3 which resulted in a vertical load of approximately 70-80kPa. The properties of Ballina clay and general site condition have been reported in detail elsewhere (Kelly et al., 2016; Pineda et al., 2016) and are summarised in Table 3. The water table is close to the ground surface. This layer of soft Ballina clay is around 10-13 metres thick and is underlain by mixture of sand and stiff clay.

Figure 10 shows a cross section of this embankment. Several settlement plates and earth pressure cells have been installed at the top surface of the central column. Differential settlement was observed between the central column and the adjacent soil surface while the stress concentration ratio was recorded by earth pressure data. The proposed model was used to make a prediction and the basic parameters are given in Table 4.

A comparison between the measurements and model predictions are shown in Figure 11. Figure 11(a) shows that the prediction for the first 50 days agrees well with the measurement; the proposed model can capture the differential settlement between column surface (S_c) and soil surface (S_s) which is missing in *equal strain* analysis, and the prediction is better when K is equal to 1000kPa. The prediction under free strain condition is not shown because there is inevitable redistribution of stress that occurs at the top of the unit cell. As for the stress concentration ratio (Figure 11b), the monitoring data were only available for the first 100 days because of the malfunctioning sensor. The measured stress concentration ratio is in the range of 2 to 3 and has a slightly increasing trend. Although the model predicted a faster increase and a higher steady value, it still provides a closer match compared to the *equal strain* condition.Figure 11 Embankment at Ballina: (a) construction order and settlement; (b) stress concentration ratio

Model limitation

Although the proposed model can provide solutions for the consolidation of soft ground improved with stone column under *equal strain*, *free strain*, and conditions in-between, by considering the foundation stiffness, there are still some inevitable limitations listed below, as also demonstrated through the case study.

(i) Shear stress would be expected at the rough column-soil interface, but complexities would arise due to the intrusion of fine particles into the column pores. The shear stress at the interface is ignored in the proposed model, so the load transfer is attributed solely to the properties of the foundation layer.

(ii) The mechanism of shear stress generation in the foundation layer is more complicated than that simplified here, i.e., the sliding surface is not vertical and highly depends on the magnitude of deformation and the types of soil.

(iii) Vertical flow in the surrounding soil is ignored, which is acceptable for a thick layer of clay, but the consolidation rate for a relatively short stone column may be underestimated.

(iv) Vertical strain in the surrounding soil is generally non-uniform (the closer to the column the less), and this is not considered in the proposed model.

Conclusions

A new consolidation model was presented to capture the consolidation of soft ground improved by stone columns under conditions ranging from *equal strain* to *free strain* by incorporating the stiffness of the foundation. The shear stress generated in the foundation layer is determined using a method similar to Terzaghi's "trapdoor theory". This method of stress redistribution is combined with consolidation to obtain generalized closed-form solutions. The derived solution was validated by comparison with previous models either under *equal strain* or *free strain*. The results showed that for stone columns, the difference between those two situations were significant and the consolidation curves corresponding to *equal strain* and *free strain* became the upper and lower boundary, respectively. It is observed that consolidation under *free strain* condition developed faster than *equal strain* initially, but then the trend reversed.

A parametric study was also carried out to examine and quantify the effect of foundation stiffness; it showed that when the stiffness of the foundation increases, (a) the time needed to achieve 90% of degree of consolidation decreases, (b) the steady stress concentration ratio increases, and (c) the differential settlement at the ground surface decreases. The influence of foundation stiffness under different modulus ratios (E_c/E_s), radius ratios (r_s/r_c), and permeability ratios (k_c/k_s) was also evaluated in this study. It was found that when the modulus ratio increases, consolidation becomes more sensitive to variations in the foundation stiffness, however, the effect of foundation stiffness on the consolidation rate is marginal under different radius ratios and permeability ratios.

An illustrative example is provided to demonstrate that the assumption of *equal strain* may lead to an overestimation of the consolidation degree in practice. Moreover, a case study at Ballina, NSW with detailed settlement and total stress measurements was also presented and analysed using the proposed model. Besides the conventional prediction of consolidation rate, additional features such as the differential settlement and the stress concentration ratio at ground surface can also be well captured. Despite of some deviation existing, it is still shown that this analytical model is capable of giving more realistic results than that under *equal strain* condition.

Acknowledgement

The authors would like to thank the financial support from the Australian Research Council (ARC) linkage project (LP130100839). The authors thank all the staff involved in the field test and their support. The first author also appreciates the helpful discussion with Dr. Rui Zhong.

References

Barron, R.A., 1948. Consolidation of Fine-Grained Soils by Drain Wells. Transactions of the American Society of Civil Engineers, 113(1): 718-742.

Bouassida, M. and Carter, J.P., 2014. Optimization of Design of Column-Reinforced Foundations. International Journal of Geomechanics: 04014031.

Chen, R., Chen, Y., Han, J. and Xu, Z., 2008. A theoretical solution for pile-supported embankments on soft soils under one-dimensional compression. Canadian Geotechnical Journal, 45(5): 611-623.

Dafalla, M.A., 2013. Effects of clay and moisture content on direct shear tests for clay-sand mixtures. Advances in Materials Science and Engineering, 2013: 1-8.

Deb, K. and Behera, A., 2016. Rate of consolidation of stone column–improved ground considering variable permeability and compressibility in smear zone. International Journal of Geomechanics, 17(6): 04016128.

Han, J., 2014. Recent research and development of ground column technologies, Proceedings of the Institution of Civil Engineers-Ground Improvement, pp. 246-264.

Han, J. and Ye, S.L., 2001. Simplified Method for Consolidation Rate of Stone Column Reinforced Foundations. Journal of Geotechnical and Geoenvironmental Engineering, 127(7): 597-603.

Hansbo, S., Jamiolkowski, M. and Kok, L., 1981. Consolidation by vertical drains. Géotechnique, 31(1): 45-66.

Hu, W., 1995. Physical modelling of group behaviour of stone column foundations. Doctoral Thesis, University of Glasgow.

Indraratna, B., Basack, S. and Rujikiatkamjorn, C., 2013. Numerical Solution of Stone Column–Improved Soft Soil Considering Arching, Clogging, and Smear Effects. Journal of Geotechnical and Geoenvironmental Engineering, 139(3): 377-394.

Ishibashi, I., 2011. Soil mechanics fundamentals. Boca Raton, FL : CRC Press, Boca Raton, FL.

Jewell, R.A., 1989. Direct shear tests on sand. Géotechnique, 39(2): 309-322.

Kelly, P., 2014. Soil Structure Interaction and Group Mechanics of Vibrated Stone Column Foundations. Doctoral Thesis, University of Sheffield.

Kelly, R.B., Pineda, J., Bates, L., Suwal, L. and Fitzallen, A., 2016. Site characterisation for the Ballina field testing facility. Géotechnique, 67(4): 279-300.

Kreyszig, E., 1988. Advanced engineering mathematics. New York : Wiley, New York.

Lei, G., Zheng, Q., Ng, C., Chiu, A. and Xu, B., 2015. An analytical solution for consolidation with vertical drains under multi-ramp loading. Géotechnique, 65(7): 531-547.

Leo, C.J., 2004. Equal strain consolidation by vertical drains. Journal of Geotechnical and Geoenvironmental engineering, 130(3): 316-327.

Low, B., Tang, S. and Choa, V., 1994. Arching in piled embankments. Journal of Geotechnical Engineering, 120(11): 1917-1938.

Lu, M.M., Xie, K.H. and Guo, B., 2010. Consolidation theory for a composite foundation considering radial and vertical flows within the column and the variation of soil permeability within the disturbed soil zone. Canadian Geotechnical Journal, 47(2): 207-217.

Madhav, M. and Van Impe, W., 1994. Load transfer through a gravel bed on stone column reinforced soil. Geotechnical Engineering, 25(2): 47-62.

Morgenstern, N. and Tchalenko, J., 1967. Microscopic structures in kaolin subjected to direct shear. Geotechnique, 17(4): 309-328.

Pineda, J., Suwal, L., Kelly, R., Bates, L. and Sloan, S., 2016. Characterisation of Ballina clay. Géotechnique, 66(7): 556-577.

Raju, V.R. and Sondermann, W., 2005. Chapter 21 Ground improvement using deep vibro techniques. In: B. Indraratna and J. Chu (Editors), Elsevier Geo-Engineering Book Series. Elsevier, pp. 601-638.

Richart, F.E., 1959. Review of the theories for sand drains. Transactions of the American Society of Civil Engineers, 124(1): 709-736.

Rujikiatkamjorn, C. and Indraratna, B., 2014. Analytical Solution for Radial Consolidation Considering Soil Structure Characteristics. Canadian Geotechnical Journal, 52(7): 947-960.

Schofield, A. and Wroth, P., 1968. Critical state soil mechanics, 310. McGraw-Hill London.

Simoni, A. and Houlsby, G.T., 2006. The direct shear strength and dilatancy of sand–gravel mixtures. Geotechnical & Geological Engineering, 24(3): 523.

Tai, P., Indraratna, B. and Rujikiatkamjorn, C., 2017. Experimental simulation and mathematical modelling of clogging in stone column. Canadian Geotechnical Journal, 55(3): 427-436.

Tang, X.W. and Onitsuka, K., 1998. Consolidation of ground with partially penetrated vertical drains. Geotechnical Engineering Journal, 29(2): 209-231.

Terzaghi, K., 1943. Theoretical soil mechanics. Wiley, New York.

Tien, H.J., 1996. A literature study of the arching effects, Massachusetts Institute of Technology.

Van Eekelen, S., Bezuijen, A. and Van Tol, A., 2013. An analytical model for arching in piled embankments. Geotextiles and Geomembranes, 39: 78-102.

Walker, R. and Indraratna, B., 2006. Vertical drain consolidation with parabolic distribution of permeability in smear zone. Journal of Geotechnical and Geoenvironmental Engineering, 132(7): 937-941.

Wang, G., 2009. Consolidation of Soft Clay Foundations Reinforced by Stone Columns under Time-Dependent Loadings. Journal of Geotechnical and Geoenvironmental engineering, 135(12): 1922-1931.

Xie, K.H., Lu, M.M. and Liu, G.B., 2009. Equal strain consolidation for stone columns reinforced foundation. International Journal for Numerical and Analytical Methods in Geomechanics, 33(15): 1721-1735.

Xu, W., Xu, Q. and Hu, R., 2011. Study on the shear strength of soil–rock mixture by large scale direct shear test. International Journal of Rock Mechanics and Mining Sciences, 48(8): 1235-1247.

Zhu, G. and Yin, J.H., 2001. Consolidation of soil with vertical and horizontal drainage under ramp load. Géotechnique, 51(4): 361-367.

Zhu, G. and Yin, J.H., 2004. Accuracy of Carrillo's formula for consolidation of soil with vertical and horizontal drainage under time-dependent loading. Communications in numerical methods in engineering, 20(9): 721-735.

Appendix I: derivation of Eqn. (6) and (7)

Combing Eqn. (3) and (4) together would yield:

$$\Delta\sigma = -\frac{r_c(r_c^2 - r_s^2)(\sigma_c - \sigma_s)}{H_1 r_s^2} \tag{a1}$$

Substitute (a1) into (5),

$$\int_0^H (\varepsilon_s - \varepsilon_c)dz = -\frac{r_c(r_c^2 - r_s^2)(\sigma_c - \sigma_s)}{K r_s^2} \tag{a2}$$

Because the stress items are independent of depth, therefore, the right side of Eqn. (a2) can be rewritten as:

$$-\frac{r_c(r_c^2 - r_s^2)(\sigma_c - \sigma_s)}{K r_s^2} = -\int_0^H \frac{r_c(r_c^2 - r_s^2)(\sigma_c - \sigma_s)}{HK r_s^2} dz \tag{a3}$$

Then Eqn. (a2) becomes an integral equation:

$$\int_0^H [(\varepsilon_s - \varepsilon_c) + \frac{r_c(r_c^2 - r_s^2)(\sigma_c - \sigma_s)}{HK r_s^2}] dz = 0 \tag{a4}$$

The integral equation usually does not have a general solving procedure, but a solution can be easily speculated.

$$(\varepsilon_s - \varepsilon_c) + \frac{r_c(r_c^2 - r_s^2)(\sigma_c - \sigma_s)}{HK r_s^2} = 0 \tag{a5}$$

Combining (a5) and (a1) gives:

$$\Delta\sigma = \frac{HK}{H_1}(\varepsilon_s - \varepsilon_c) \tag{a6}$$

Substituting Eqn. (a6) into Eqns. (3) and (4) would yield:

$$\sigma_s = \sigma + \frac{Kr_cH(\varepsilon_s - \varepsilon_c)}{{r_c}^2 - {r_s}^2} \tag{a7}$$

$$\sigma_c = \sigma + \frac{KH(\varepsilon_s - \varepsilon_c)}{r_c} \tag{a8}$$

Take derivative of (a7) and (a8) with respect to time, *t*, and combining with Eqn. (1) leads to:

$$\frac{\partial \varepsilon_s}{\partial t} = \frac{m_{vs}[HKr_c\frac{\partial \varepsilon_c}{\partial t} + \frac{\partial \bar{u}_s}{\partial t}(r_c^2 - r_s^2)]}{m_{vs}HKr_c - r_c^2 + r_s^2} \tag{a9}$$

$$\frac{\partial \varepsilon_c}{\partial t} = \frac{m_{vc}(HK\frac{\partial \varepsilon_s}{\partial t} - \frac{\partial \bar{u}_c}{\partial t}r_c)}{m_{vc}HK + r_c} \tag{a10}$$

Combining (a9) and (a10), then Eqn. (6) and (7) can be obtained.

Appendix II: derivation of Eqn. (15)

Integrating Eqn. (8) considering the radius from r to r_s, and then combining Eqn. (10) yields:

$$\frac{\partial u_s}{\partial r}=\frac{\gamma_w(r_s^2-r^2)}{2k_s f(r)r}\frac{\partial \varepsilon_s}{\partial t} \tag{b1}$$

Substituting (b1) into (9) gives:

$$\frac{r_s^2-r_c^2}{r_c^2}\frac{\partial \varepsilon_s}{\partial t}+\frac{k_c}{\gamma_w}\frac{\partial^2 \bar{u}_c}{\partial z^2}=-\frac{\partial \varepsilon_c}{\partial t} \tag{b2}$$

Integrating (b1), the following equation can be derived by incorporating (11), thus,

$$u_s-\bar{u}_c=\frac{\gamma_w}{2k_s}\frac{\partial \varepsilon_s}{\partial t}\int_{r_c}^{r}\frac{r_s^2-r^2}{f(r)r}dr \tag{b3}$$

A relationship can also be established between the average pore water pressure in the surrounding clay and the pore pressure in the stone column, as given in (b4) and (b5).

$$\bar{u}_s=\frac{1}{\pi(r_s^2-r_c^2)}\int_{r_c}^{r_s}2\pi r u_s dr=\bar{u}_c+\frac{\gamma_w A}{k_s(r_s^2-r_c^2)}\frac{\partial \varepsilon_s}{\partial t} \tag{b4}$$

$$A=\int_{r_c}^{r_s}r\int_{r_c}^{r}\frac{r_s^2-r^2}{f(r)r}dr\,dr \tag{b5}$$

Combining (6) with (b4) and (b5) gives:

$$\bar{u}_s=\bar{u}_c+B\frac{\partial \bar{u}_c}{\partial t}+C\frac{\partial \bar{u}_s}{\partial t} \tag{b6}$$

$$B=-\frac{m_{vc}m_{vs}AKHr_c^2\gamma_w}{k_s(r_c^2-r_s^2)[Km_{vc}H(r_c^2-r_s^2)+r_c(r_c^2-r_s^2)-KHr_c m_{vs}]} \tag{b7}$$

$$C = -\frac{A(KHm_{vc}m_{vs} + m_{vs}r_c)\gamma_w}{k_s[Km_{vc}H(r_s^2 - r_c^2) + m_{vs}KHr_c^2 + r_c(r_s^2 - r_c^2)]} \tag{b8}$$

Then substituting (6) and (7) into (b2) gives:

$$\frac{\partial \bar{u}_s}{\partial t} = D\frac{\partial \bar{u}_c}{\partial t} + E\frac{\partial^2 \bar{u}_c}{\partial z^2} \tag{b9}$$

$$D = \frac{r_c^2[m_{vc}r_c(r_c^2 - r_s^2) - m_{vc}m_{vs}KHr_s^2]}{(r_c^2 - r_s^2)[m_{vs}r_c(r_c^2 - r_s^2) - m_{vc}m_{vs}KHr_s^2]} \tag{b10}$$

$$E = -\frac{k_c r_c^2[Km_{vc}H(r_c^2 - r_s^2) + r_c(r_s^2 - r_c^2) - m_{vs}KHr_c^2]}{\gamma_w(r_c^2 - r_s^2)[m_{vs}r_c(r_c^2 - r_s^2) - m_{vc}m_{vs}KHr_s^2]} \tag{b11}$$

Substituting (b9) into (b6) leads to:

$$\bar{u}_s = \bar{u}_c + (B + CD)\frac{\partial \bar{u}_c}{\partial t} + CE\frac{\partial^2 \bar{u}_c}{\partial z^2} \tag{b12}$$

Taking the derivative of Eqn. (b12) with respect to time, and then combining with Eqn. (b9) to eliminate the item involving $\bar{u}_s$, allows one to obtain the governing equation (15).

List of Tables

Table 1 Basic parameters used in analysis (Indraratna et al. 2013)

k_s(m/s)	k_c/k_s	r_c(m)	r_s(m)	r_d/r_c
1.6×10^{-9}	10^3	0.5	1.5	1.15
k_d/k_s	**M(m_{vs}/m_{vc})**	**γ_w(kN/m^3)**	**H(m)**	**m_{vs}(MPa^{-1})**
0.1	7	10	16	2

Table 2 Foundation stiffness for different geo-materials based on direct shear tests

Sources	**Soil Type**	**Shear rate(mm/s)**	**Specimen dimension(mm)**	**Normal stress (kPa)**	**Corresponding K* (kPa)**
Xu et al. (2011)	Soil-rock mixture	0.1-0.133	600x600x400	10-40	400-3000
Dafalla (2013)	Clay-sand mixture	0.002	100x100	49-147	3000-10000
Simoni and Houlsby (2006)	Sand-gravel mixture	0.0056	254x152x150	90	1000-5000
Jewell (1989)	Sand	-	250x152x152	30-33	4000-11000
Morgenstern and Tchalenko (1967)	Clay	0.000049	60x60x25	215	11000-18000

*Estimated based on the shear stress-horizontal displacement curves in the literature

Table 3 Properties of Ballina clay (Pineda et al. 2016)

Borehole number	Inclo2	Mex9
Depth	2.1m-10.5m	2.8m-10m
Water content	78%-122%	81%-113%
Liquid limit	87%-128%	87%-127%
Plastic limit	32%-50%	34%-46%
Initial void ratio e_0	2.03-3.31	2.16-2.89
Dry density ρ_d (g/cm^3)	0.62-0.89	0.65-0.87
Coefficient of consolidation c_v (m^2/year)	2.5-285.9	4.75-23.5
Undrained shear strength s_u (kPa)	11-24	10-26
Permeability k (10^{-9}m/s)	0.65-54	0.5-4.7
Modulus M (kPa)	1140-2561	1587-3120

Table 4 Parameters used in prediction of field embankment

H(m)	**r_s(m)**	**r_c(m)**	**r_d/r_c**	**K(kPa)**
10	1.13	0.4	[b]1.15	[c]500/1000
k_s(m/s)	**k_c(m/s)**	**k_d/k_s**	**m_{vs}/m_{vc}**	**m_{vs}(MPa^{-1})**
[a]10^{-9}	[b]10^{-4}	[b]0.1	[b]10	[a]0.7

a. based on results of Pineda et al. (2016) and Kelly et al. (2017)
b. according to Han and Ye (2001), Indraratna et al. (2013)
c. Assumed based on Table 2

List of Figures

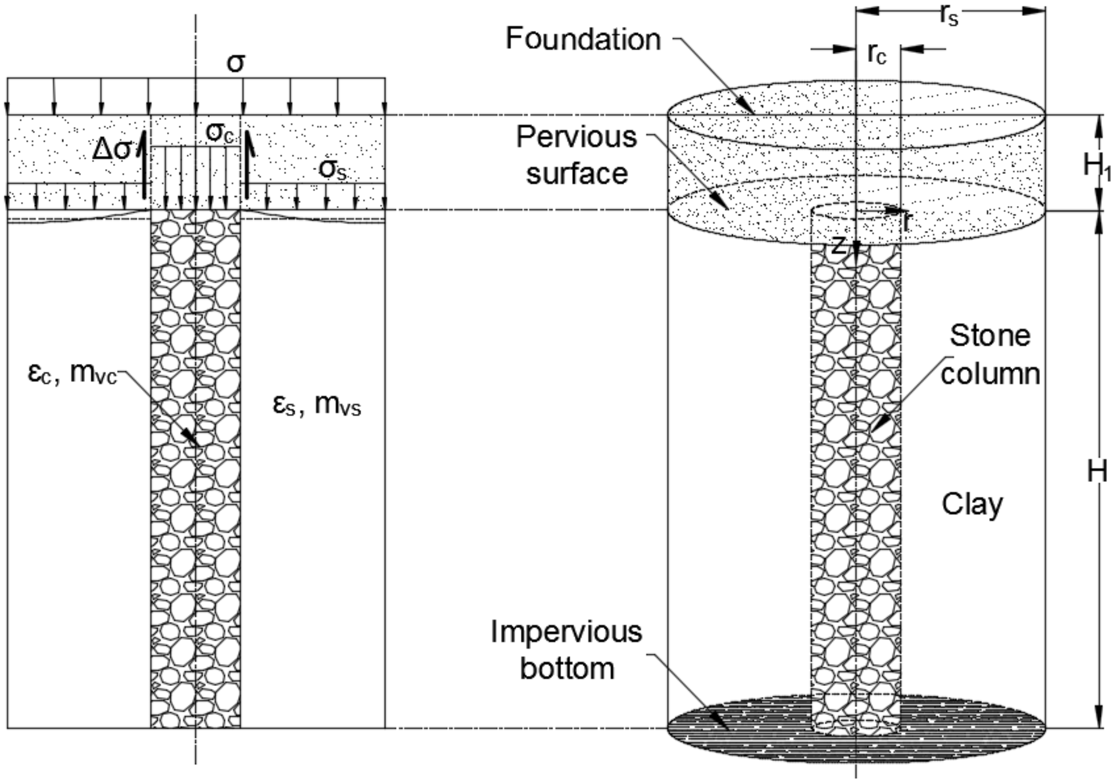

Figure 1 A stone column unit cell

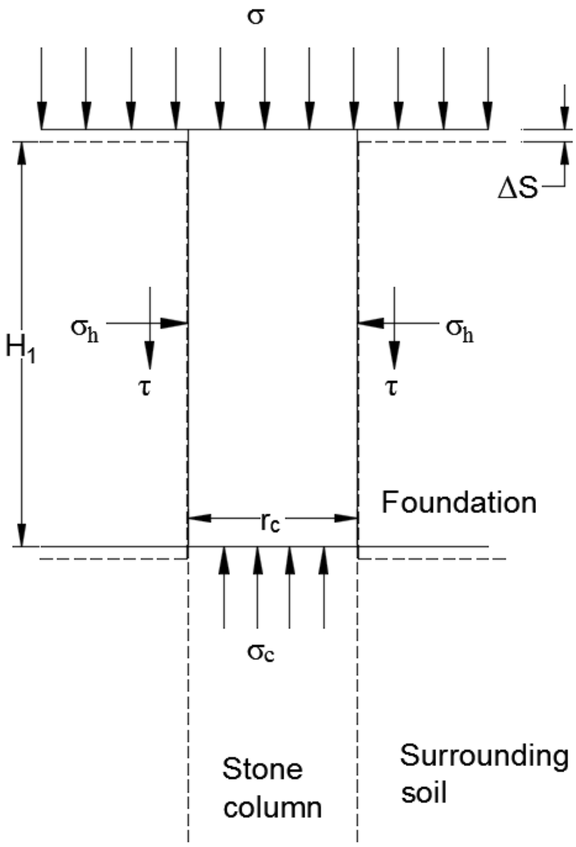

(a)

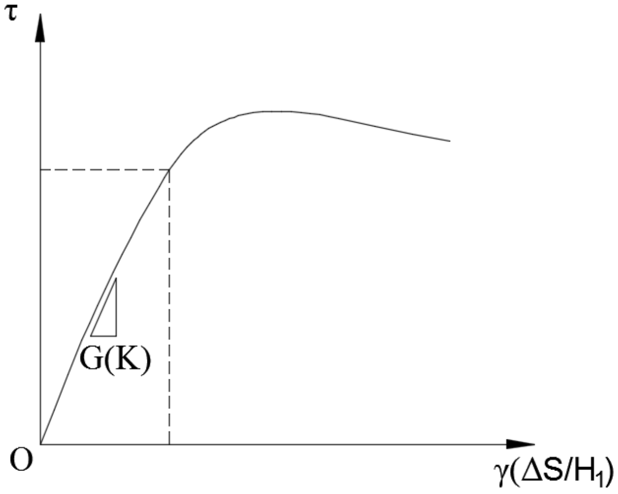

(b)

Figure 2 Shear stress in the foundation layer (a) trapdoor theory (Terzaghi 1943); (b) typical stress-strain relationship (based on direct shear test)

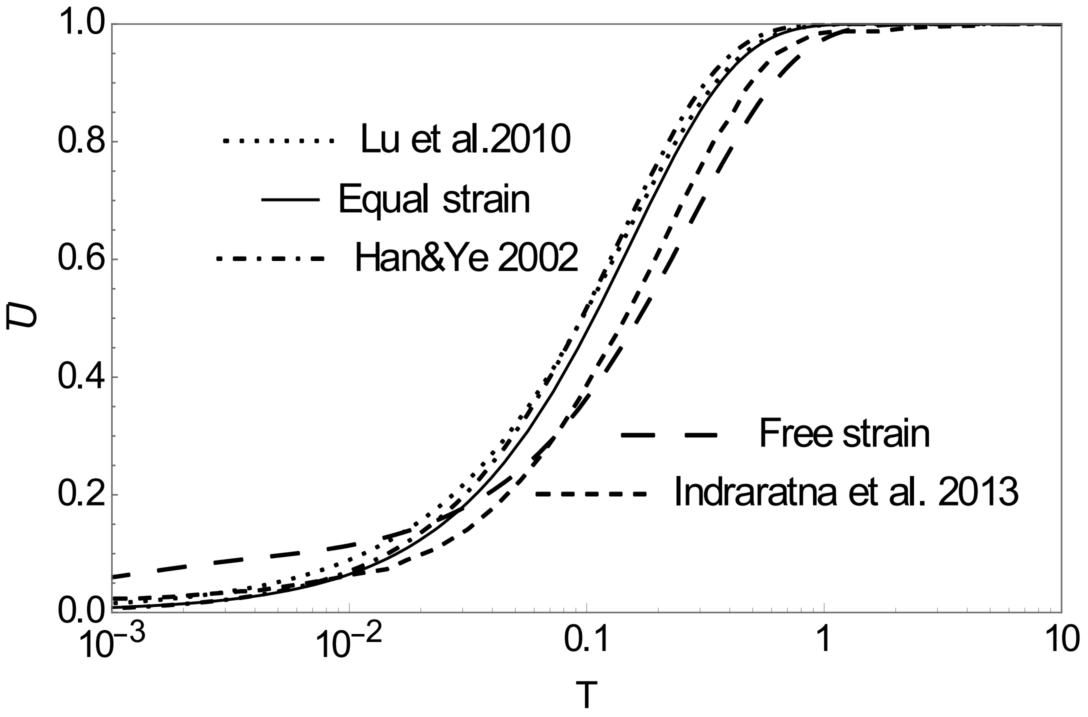

Figure 3 Comparison between proposed model and previous models

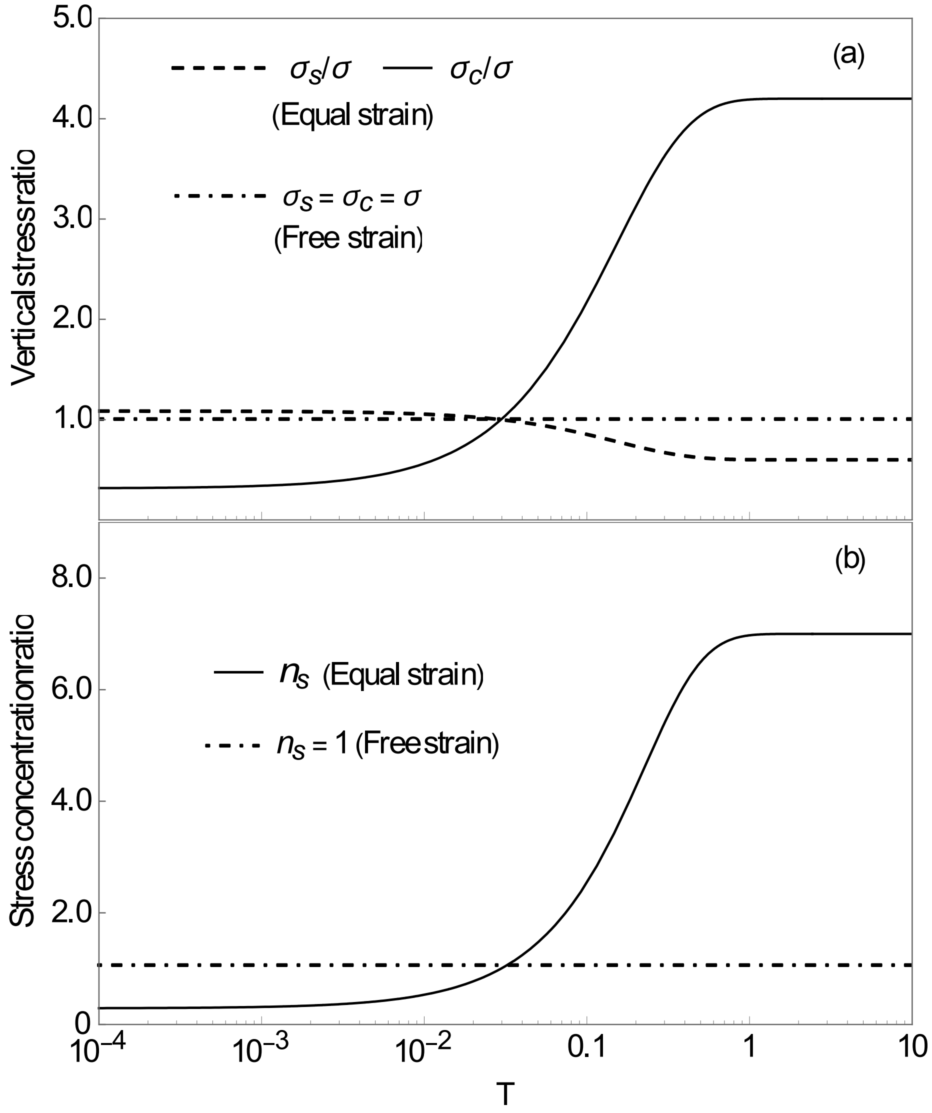

Figure 4 Vertical stress on top of the unit cell: (a) vertical stress ratio; (b) stress concentration ratio

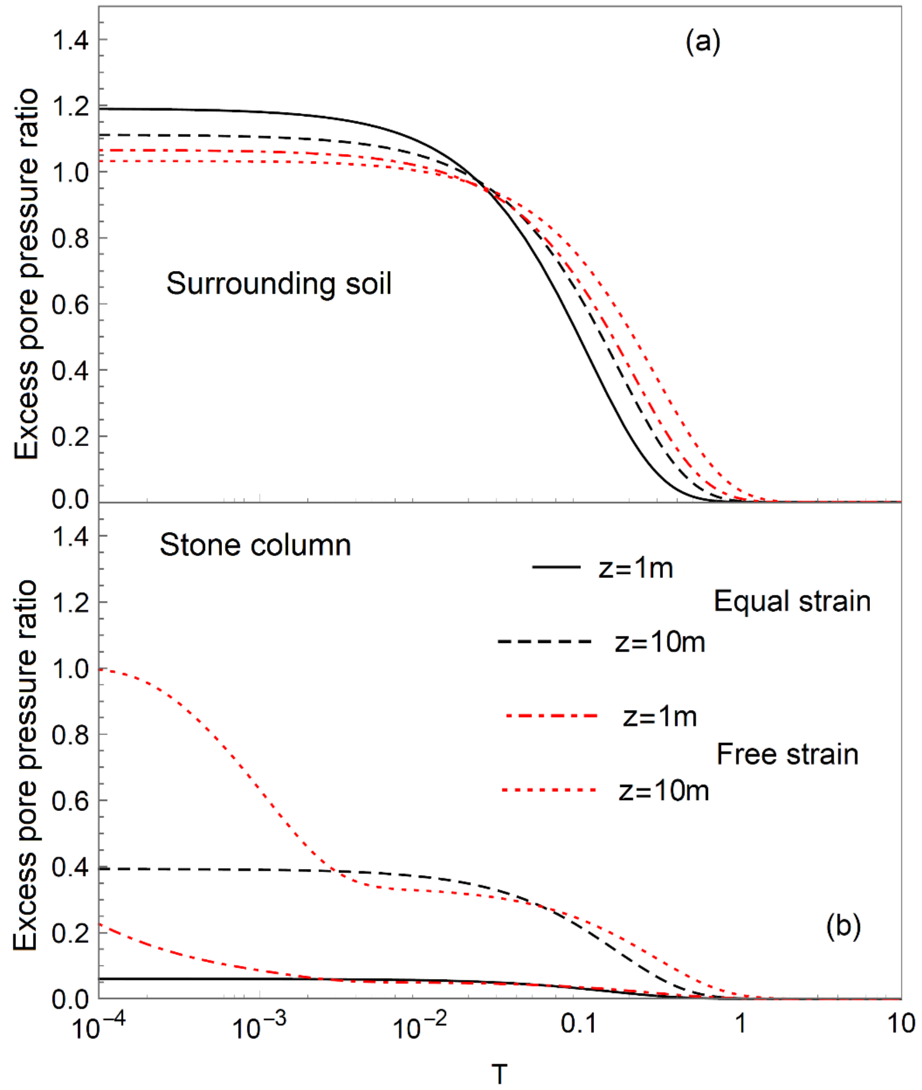

Figure 5 Development of excess pore pressure for equal strain and free strain (depth of 1m and 10m): (a) surrounding soil; (b) stone column

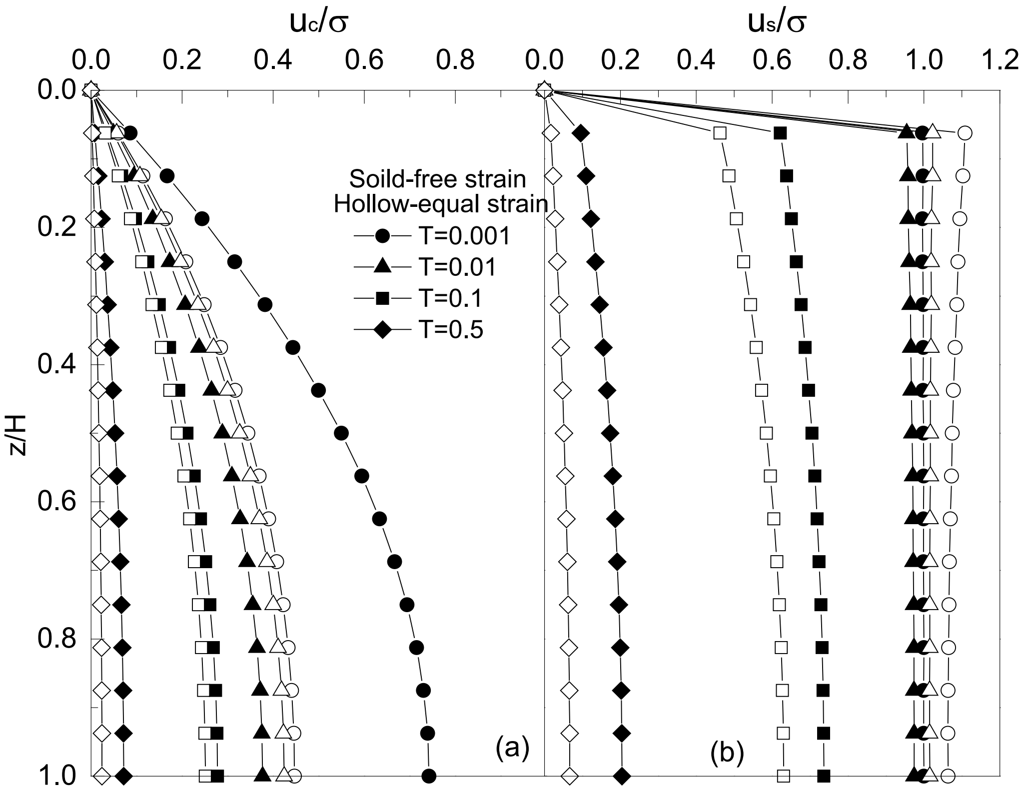

Figure 6 Excess pore pressure profiles: (a) in stone column; (b) in surrounding soil

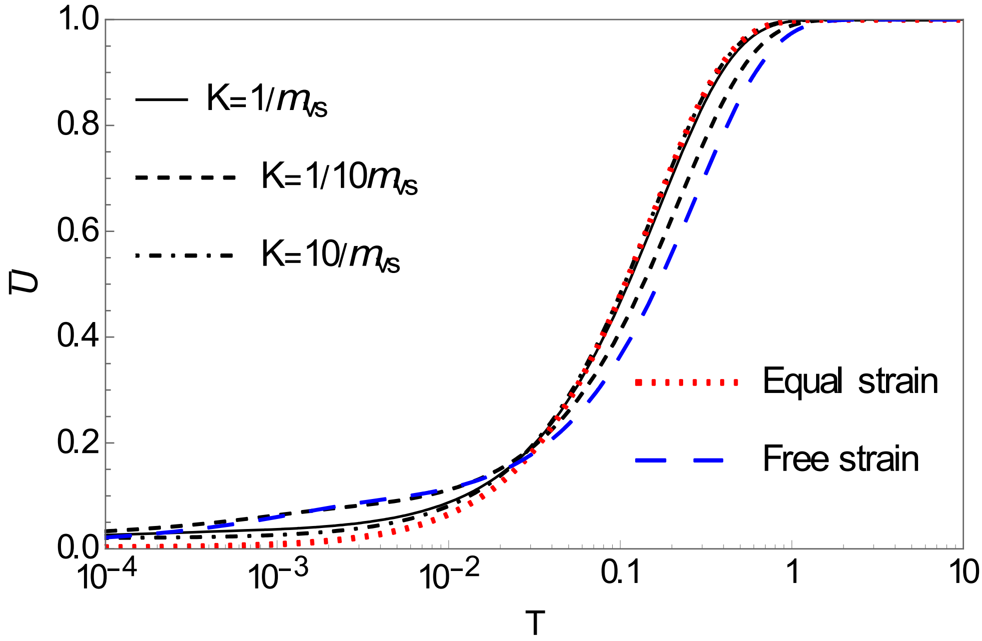
K=1/mvs
K=1/10mvs
K=10/mvs
Equal strain
Free strain
Ū
T
1.0
0.8
0.6
0.4
0.2
0.0
10−4
10−3
10−2
0.1
1
10

(a)

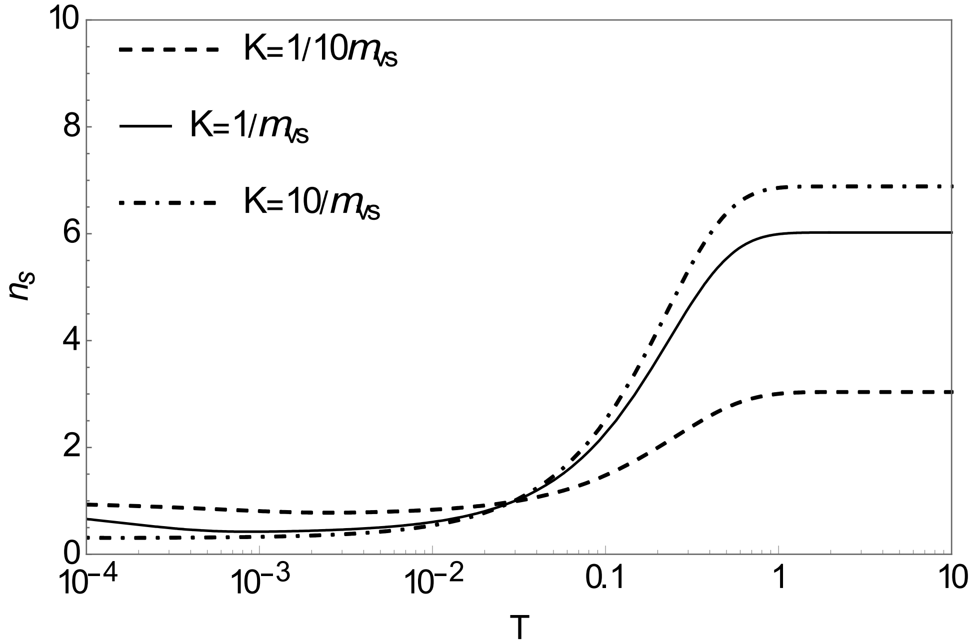
K=1/10mvs
K=1/mvs
K=10/mvs
ns
T
10
8
6
4
2
0
10−4
10−3
10−2
0.1
1
10

(b)

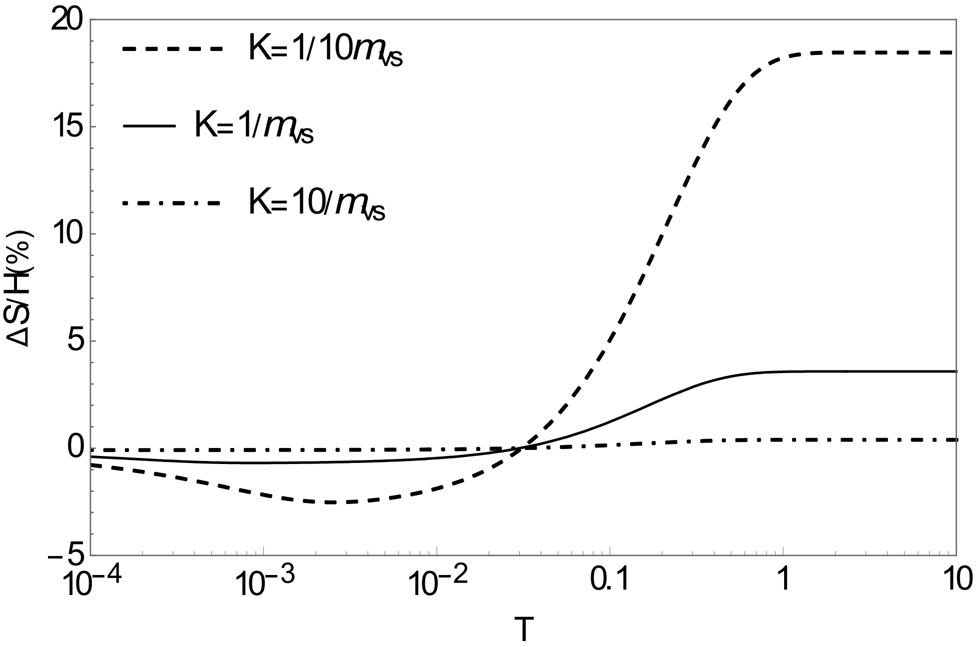

(c)

Figure 7 Effect of foundation stiffness on: (a) average degree of consolidation; (b) stress concentration ratio; (c) differential settlement

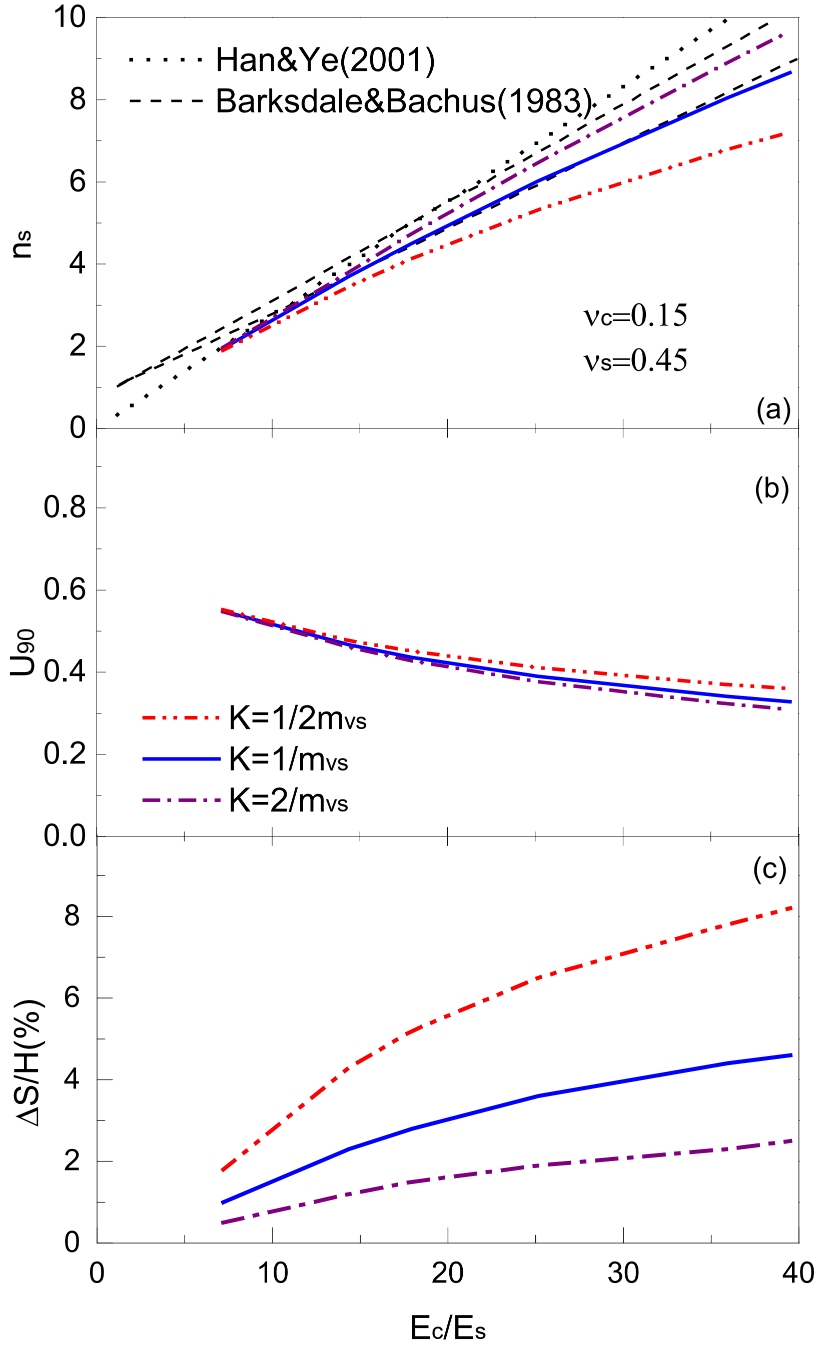

Figure 8 Effect of modulus ratio under varying foundation stiffness: (a) steady stress concentration ratio (n_s); (b) time to achieve 90% degree of consolidation (U_{90}); (c) differential settlement ratio ($\Delta S/H$)

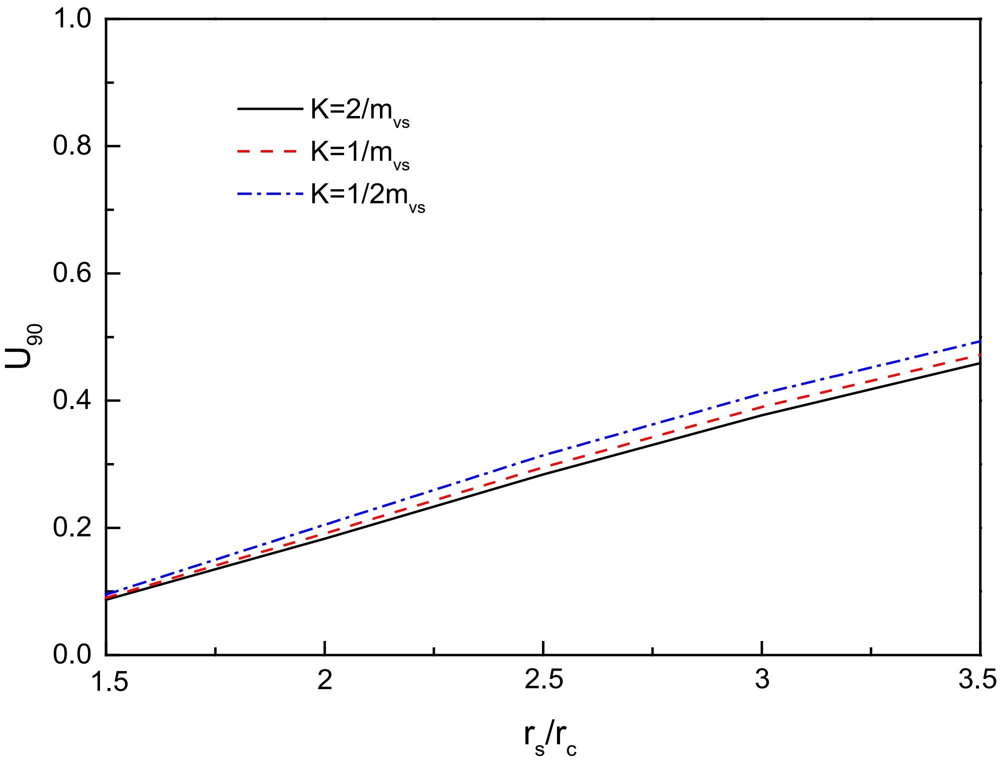

(a)

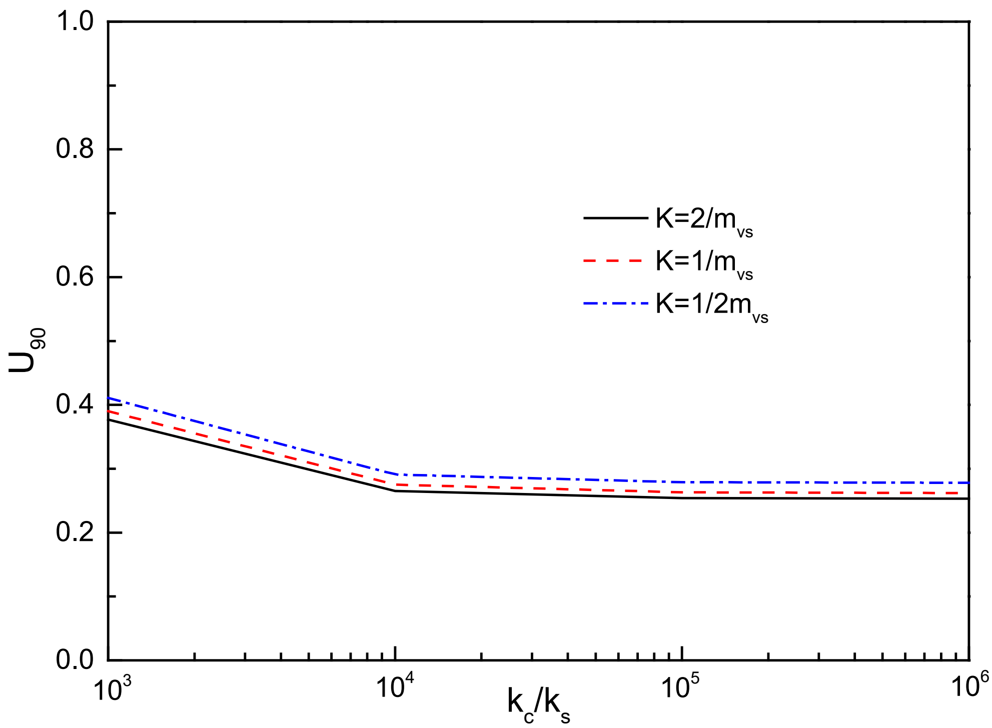

(b)

Figure 9 Effect of foundation stiffness on U_{90}: (a) radius ratio (r_s/r_c); (b) permeability ratio (k_c/k_s)

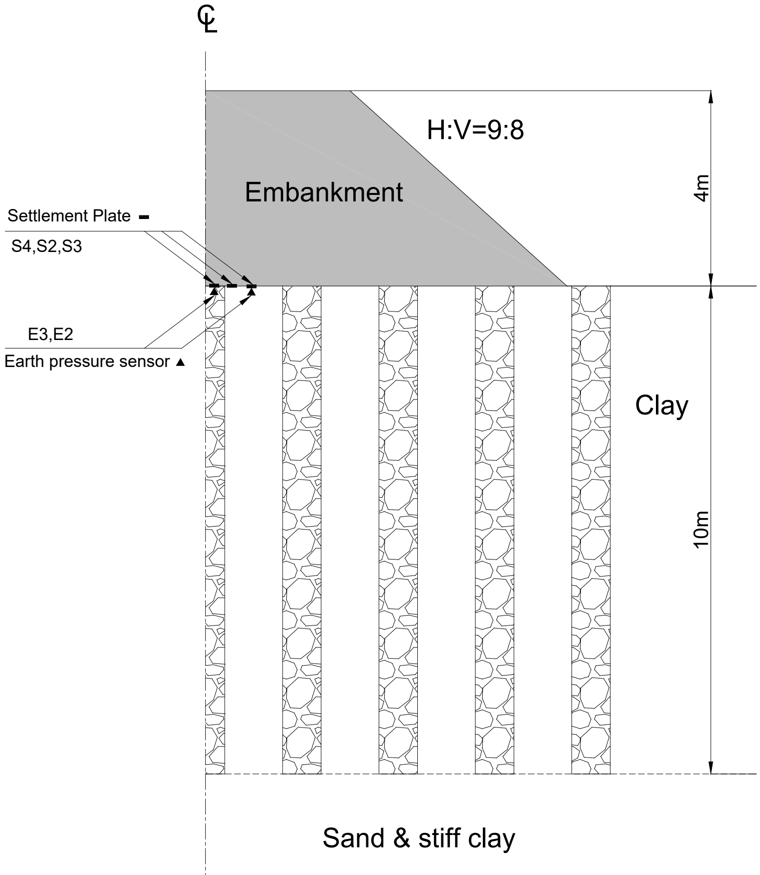

Figure 10 Cross-section of embankment beyond stone columns

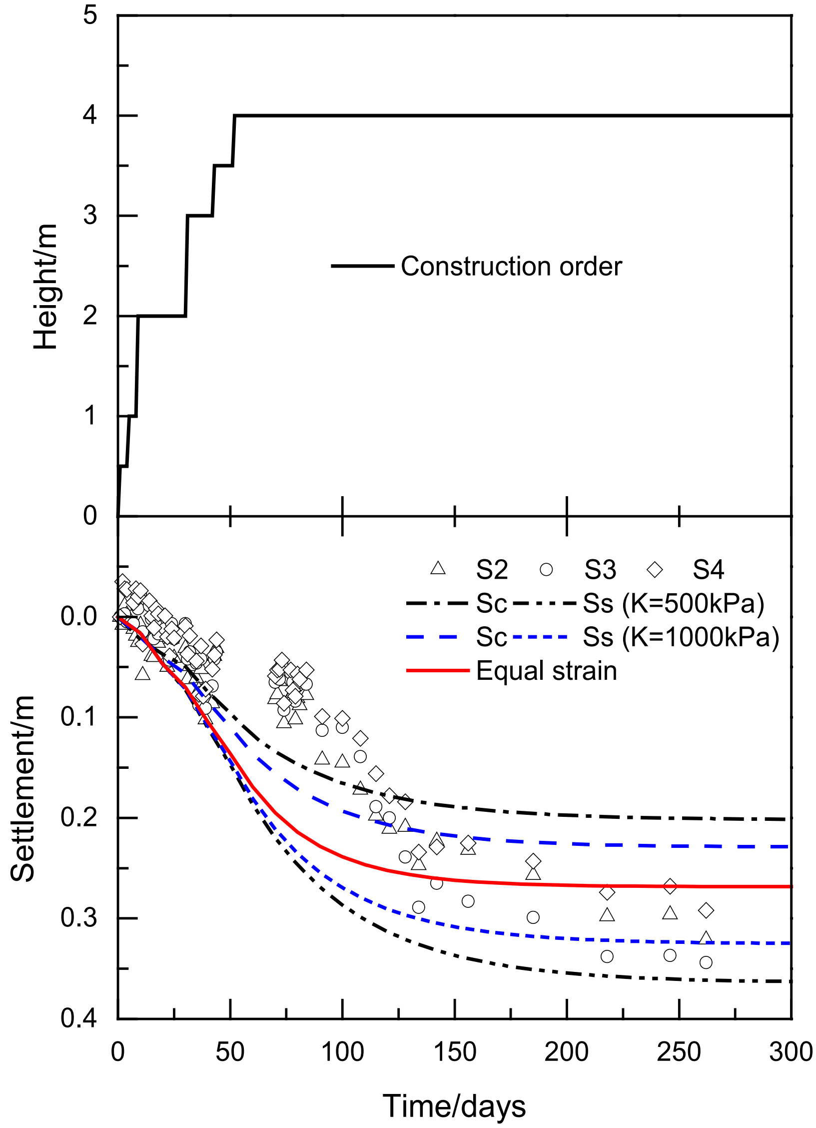
Height/m
Construction order
Settlement/m
S2
S3
S4
Sc
Ss (K=500kPa)
Sc
Ss (K=1000kPa)
Equal strain
Time/days

(a)

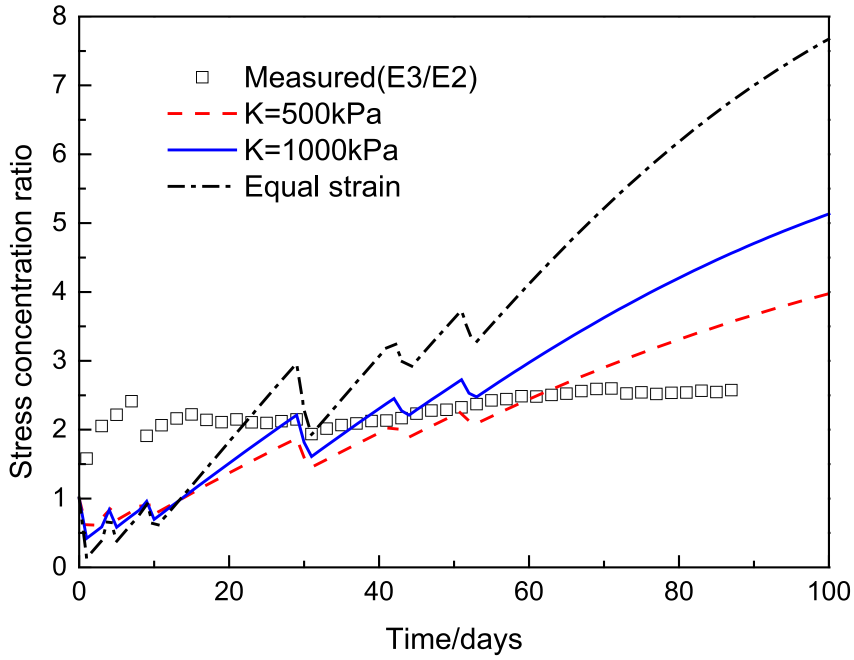

(b)

Figure 11 Embankment at Ballina: (a) construction order and settlement; (b) stress concentration ratio